Title

Dopamine D3 receptor binding of 18F-fallypride: Evaluation using in vitro and in vivo PET imaging studies

Journal
Synapse, 69(12)

ISSN
0887-4476

Authors
Mukherjee, Jogeshwar
Constantinescu, Cristian C
Hoang, Angela T
et al.

Publication Date
2015-12-01

DOI
10.1002/syn.21867

Peer reviewed

Published in final edited form as:
Synapse. 2015 December ; 69(12): 577–591. doi:10.1002/syn.21867.

Dopamine D3 receptor binding of ¹⁸F-Fallypride: Evaluation using *in vitro* and *in vivo* PET imaging studies

Jogeshwar Mukherjee[1], **Cristian C. Constantinescu**[1], **Angela T. Hoang**[1], **Taleen Jerjian**[1], **Divya Majji**[1], and **Min-Liang Pan**[1]

[1]Preclinical Imaging, Department of Radiological Sciences, University of California, Irvine, CA 92697

Abstract

Identification of dopamine D3 receptors (D3R) *in vivo* is important to understand several brain functions related to addiction. The goal of this work was to identify D3R binding of the dopamine D2 receptor (D2R)/D3R imaging agent, ^{18}F-fallypride. Brain slices from male Sprague-Dawley rats (n=6) and New Zealand White rabbits (n=6) were incubated with ^{18}F-fallypride and D3R selective agonist (*R*)-7-OH-DPAT (98-fold D3R selective). Rat slices were also treated with BP 897 (68-fold D3R selective partial agonist) and NGB 2904 (56-fold D3R selective antagonist). *In vivo* rat studies (n=6) were done on Inveon PET using 18–37 MBq ^{18}F-fallypride and drug-induced displacement by (*R*)-7-OH-DPAT, BP 897 and NGB 2904. PET/CT imaging of wild type (WT, n=2) and D2R knock-out (KO, n=2) mice were carried out with ^{18}F-fallypride. (*R*)-7-OH-DPAT displaced binding of ^{18}F-fallypride, both *in vitro* and *in vivo*. *In vitro*, at 10 nM (*R*)-7-OH-DPAT, ^{18}F-fallypride binding in the rat ventral striatum (VST) and dorsal striatum (DST) and rabbit nucleus accumbens were reduced by ~10–15%. At 10 μM (*R*)-7-OH-DPAT all regions in rat and rabbit were reduced by ≥85%. *In vivo* reductions for DST and VST before and after (*R*)-7-OH-DPAT were: low-dose (0.015mg/kg) DST −22%, VST −29%; high-dose (1.88 mg/kg) DST −58%, VST −77%, suggesting D_3R/D_2R displacement. BP 897 and NGB 2904 competed with ^{18}F-fallypride *in vitro*, but unlike BP 897, NGB2904 did not displace ^{18}F-fallypride *in vivo*. The D2R KO mice lacked ^{18}F-fallypride binding in the DST. In summary, our findings suggest that up to 20% of ^{18}F-fallypride may be bound to D3R sites *in vivo*.

Graphical Abstract

Corresponding author: Jogeshwar Mukherjee, Ph.D., Department Radiological Sciences, University of California Irvine, Medical Sciences B, B-138, Irvine, CA 92697-5000, Phone: +1 949 824 2018, Fax: +1 949 824 2344, j.mukherjee@uci.edu.

Conflict of Interest

The authors declare no conflict of interest in the work presented here.

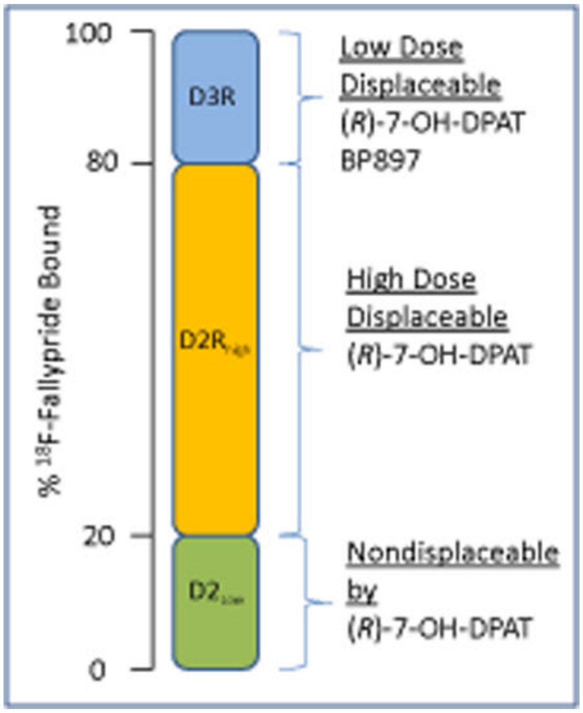

Keywords

^{18}F-Fallypride; Dopamine D3 Receptors; PET Imaging; 7-OH-DPAT; BP 897; NGB 2904; Addiction

1. Introduction

Dopamine D3 receptors (D3R) (Sokoloff et al., 1990) are D2-like receptors and are considered to be involved in functions of the mesolimbic dopaminergic system such as reward and reinforcement and in the pathology of addiction (Heidbreder et al., 2005). The D3R mRNA is widely distributed in the rodent brain with D3Rs having a function in neuronal pathways linked to the intoxication stage of drug addiction (Koob and Le, 1997; Everitt and Robbins, 2005), the craving stage of drug-seeking behavior induced by drugs, potential therapeutic target for addiction (Paterson et al., 2014), drug cues and stress (McFarland and Kalivas, 2011; Everitt and Wolf, 2002; Shaham et al., 2003), and compulsive behaviors (Koob and Le, 1997; Everitt and Robbins, 2005). Agonists that bind only to the functional state (high-affinity state) of the receptors are more amenable for substance abuse studies in order to better understand drug addiction (Le Foll et al., 2014).

^{18}F-Fallypride is an antagonist radioligand with high affinity for dopamine D2 receptors (D2R) and D3R and exhibits binding which allows quantitation of receptor densities in striatal and extrastriatal regions. Binding of ^{18}F-fallypride has been demonstrated through positron emission tomography (PET) studies in rodents, non-human primates and humans (Christian et al., 2009; Constantinescu et al., 2011; Mukherjee et al., 2002; Rominger et al., 2010; Slifstein et al., 2004; Tantawy et al., 2009). *In vitro* ^{18}F-fallypride presents similar affinities for both D2R and D3R ($D2R_{Short}$ K_i = 2.1 nM, $D2R_{Long}$ K_i = 2.2 nM, D3 K_i = 1.6 nM (Stark et al., 2007) with ^{3}H-spiperone). The D3R binding component of ^{18}F-fallypride has not been clearly elucidated *in vitro* or *in vivo*.

In vivo PET imaging with selective D3R radiotracers may facilitate studies in animal models aimed at elucidating the specific role of D3Rs in various brain regions, which so far has been mostly limited to micro infusion of dopamine D3 antagonists into the rodent brains (Xi et al., 2013; Loiseau & Millan, 2009; McFarland et al., 2004). There has been a continuing interest in developing PET tracers that specifically target D3R, however, the tracers synthesized so far have affinity for both D2R and D3R subtypes. One promising and utilized PET tracer is ^{11}C-(+)-PHNO, a dual D3R/D2R agonist with higher affinity for D3R over D2R *in vivo*. ^{11}C-(+)-PHNO has been shown to present preferential uptake in D3R rich regions such as ventral striatum, globus pallidus, and substantia nigra in humans and non-human primates (Narendran et al., 2006; Gallezot et al., 2012, Ginovart et al., 2006; Graff-Guerrero et al., 2008). Baboon studies have demonstrated that the specific binding of ^{11}C-(+)-PHNO has been inhibited by BP 897 (partial D3 receptor agonist), showing the D3R component of the PET signal (Narendran et al., 2006). In addition to non-human primates, *ex vivo* autoradiographic studies in D2R and D3R knockout mice have also been conducted (Rabiner et al., 2009). Blockade studies of ^{11}C-(+)-PHNO in humans with D3R antagonist ABT-925 have shown that most blocking occurred in the substantia nigra and ventral striatum, regions rich in D3R (Graff-Guerrero et al., 2010). Despite its high *in vivo* selectivity for D3R, the binding of ^{11}C-(+)-PHNO to D2R cannot be neglected and methodology has been proposed to separate the fractional D3R versus D2R *in vivo* binding of ^{11}C-(+)-PHNO in rhesus monkeys and humans (Gallezot et al., 2012; Tziortzi et al., 2011).

The goal of this work was to assess the relative proportion of D3R binding of ^{18}F-fallypride. Thus, in an effort to differentiate this D3R binding of ^{18}F-fallypride, following sets of experiments were carried out: 1. *In vitro* autoradiographic studies with ^{18}F-fallypride and competition with various D3R–selective drugs, 7-OH-DPAT, D3R agonist (Davoodi et al., 2014), in the rat and rabbit brain and BP897 and NGB2904in rat brain (Table 1). 2. PET studies in rats with ^{18}F-fallypride under baseline and D3R–selective drug competition at different doses. 3. PET studies in wild type (WT) and D2R deficient homozygous (D2R KO) mice with ^{18}F-fallypride. Our assumption was that the observed binding of ^{18}F-fallypride in the KO mice may be attributed entirely to D3R, with the difference between the WT and KO being attributed to the D2R binding components of these radioligands.

2. Materials and Methods

2.1 General Methods

All chemicals and solvents were of analytical or HPLC grade from Aldrich Chemical Co. and Fisher Scientific. High specific activity ^{18}F-fluoride was produced in the MC-17 cyclotron using oxygen-18 enriched water (^{18}O to ^{18}F using p, n reaction). The high specific activity ^{18}F-fluoride was used in subsequent reactions which were carried out in automated radiosynthesis units (chemistry processing control unit (CPCU)). Semi-preparative reverse-phase separation using C18 columns was carried out on Gilson high performance liquid chromatography (HPLC) system. Fluorine-18 radioactivity was counted in a Capintec CRC-15R dose calibrator while low level counting was carried out in a Capintec Caprac-R well-counter. Brain tissue was sectioned in a Leica Cryotome. Fluorine-18 autoradiographic studies were carried out by exposing tissue samples on storage phosphor screens (Perkin Elmer Multisensitive, Medium MS). The apposed phosphor screens were read and analyzed by OptiQuant acquisition and analysis program of the Cyclone Storage Phosphor System (Packard Instruments Co., Boston, MA). A preclinical Inveon dedicated PET scanner (Siemens Medical Solutions, Knoxville, TN) with a transaxial full width half maximum (FWHM) of 1.46 mm, and axial FWHM of 1.15 mm (Constantinescu and Mukherjee, 2009) was used for the PET studies. PET images were analyzed using PMOD software. All animal studies were approved by the University of California Irvine Institutional Animal Care and Use Committee (UCI IACUC).

2.2 ^{18}F-Fallypride Synthesis

The synthesis of ^{18}F-fallypride was carried out using previously reported methods (Mukherjee et al., 1995). ^{18}F-Fallypride was typically obtained in specific activity >74 MBq/nmol in approximately 370 MBq batches for imaging studies. The final sterile 0.9% saline solution of ^{18}F-fallypride, pH in the range of 6–7, was dispensed for *in vitro* and *in vivo* studies.

2.3 *In Vitro* Studies

Male Sprague-Dawley rats (250–300g; n=6) and White New Zealand rabbits (~4 kg; n=6) were anesthetized and decapitated; the brain was rapidly removed and frozen in isopentane at −20 °C. Brain slices 10 μm thick contained regions known to have dopamine receptors which include the striata, hippocampus, cortex and cerebellum as a reference region. Brain slices were pre-incubated in Tris buffer (50 mM Tris HCl, 2.5 mM $CaCl_2$, 125 mM NaCl, 1 mM MgCl, 5 mM KCl, 0.l mM sodium ascorbate, pH 7.4) at room temperature for 10 minutes. The slides were incubated in the buffer at room temperature for 10 minutes and then in buffer with 111 kBq/cc ^{18}F-fallypride at 37 °C for 1 hr. Nonspecific binding was measured in the presence of 10 μM sulpiride. After incubation, slides were washed twice (each wash lasting one minute) with ice-cold buffer. Slides were then quickly dipped in cold deionized water, air dried, and exposed to a phosphor screen for 24 hours. The amount of binding was evaluated in digital light units (DLU/mm^2).

A similar protocol was used to measure drug effects of 7-OH-DPAT, BP 897 and NGB 2904. Horizontal rat brain slices were used in competition experiments carried out with 7-OH-DPAT at concentration ranging between 1 nM and 10 μM. Sagittal rat and rabbit brain slices were used to measure and compare the effects of 7-OH-DPAT, BP 897 and NGB 2904. After incubation, slides were washed twice in cold buffer and a third time in cold millipore water. The slides were then dried, and exposed to phosphor film. The exposed films were quantified with OptiQuant software and rat brain regions of interest including the dorsal striatum, ventral striatum, and cerebellum as reference for non-specific binding were identified using the rat brain atlas (Paxinos and Watson, 1998). Data was analyzed using following procedure: (a) the non-specific binding of ^{18}F-fallypride was subtracted for all samples; (b) the specific binding was normalized to 100% (no competitive ligand) and (c) the binding isotherms were fit to the Hill equation (KELL BioSoft software (v 6), Cambridge, U.K.) to provide the half maximal inhibitor concentration (IC_{50}) values. (d) the competition curves were plotted using GraFit data analysis (Erithacus Software, Inc).

2.4 *In Vivo* Rat PET Studies

Male Sprague-Dawley rats (250–300 g; n=6) were fasted 24 hours prior to time of scan. On the day of the study, rats were anesthetized using 4.0% isoflurane. The rats were then positioned on the scanner bed by placing it on a warm-water circulating heating pad and anesthesia applied using a nose-cone. ^{18}F-Fallypride (18–37 MBq) was injected intravenously in the tail as 0.3 mL bolus. Isoflurane was reduced and maintained at 2.5% following injection. Scans were carried out for 180 minutes and acquired by the Inveon PET in full list mode. Drugs were administered 90 minutes post-injection of ^{18}F-fallypride. In separate trials with the same animal, four different doses of (*R*)-7-OH-DPAT were administered: 0.015 mg/kg, 0.06 mg/kg, 0.38 mg/kg and 1.88 mg/kg. Two other rats received similar ^{18}F-fallypride scans, during which NGB 2904 and BP 897 were injected at 90 minutes post-injection of ^{18}F-fallypride. NGB 2904 and BP 897 drug solutions were prepared using 2-hydroxypropyl-β-cyclodextrin (HPbCD) due to their low water solubility according to the reported protocols for NGB 2904 (Xi et al., 2004) and for BP 897 (Gilbert et al. 2005). NGB 2904 was administered at a dose of 4 mg/kg in 5% HPbCD solution and BP 987 was administered at a dose of 3.2 mg/kg in 25% HPbCD solution.

The images were reconstructed using Fourier rebinning and 2D OSEM method with an image matrix of 128×128x159, resulting in a pixel size of 0.77 mm and a slice thickness of 0.796 mm. All dynamic images were corrected for radioactive decay. Attenuation correction was performed using a 10-min transmission scan with a ^{57}Co point source prior to tracer injection. Images were corrected for scatter and photon attenuation using data from a 20 min transmission scan with a Co-57 point source. The list-mode data were rebinned into 3D sinograms of span 3 and ring difference 79. Random events were subtracted prior to reconstruction. The data from 0–90 min acquisition was histogrammed in 30 time frames and the data from 90 min acquisition was histogrammed into 18 frames of 5 min each. Calibration in Bq/cc units was applied using a Ge-68 phantom which was scanned and reconstructed under the same parameters as the subjects.

PMOD software was used to process images, extract and analyze time-activity curves from regions of interest drawn on the dorsal striatum, ventral striatum, and cerebellum, which was used as reference for non-specific binding.

2.5 *In Vivo* Mice PET Studies

All mice for this study were bred and genotyped prior to their use in imaging. D2R knock-out mice were generated following an established procedure (Baik et al., 1995; Boulay et al., 1999). Mice were housed in individual cages, kept in a climate controlled room (24.4°C), with a 12:12-hour light cycle, and had free access to food and water during housing. Subjects were fasted in the imaging room, in a dark quiet place, for 24 hours prior to the start of experiments with ^{18}F-fallypride. Two wild-type (WT) C57BL/6 mice and two D2 knock-out (D2 KO) mice (male, 30–35 g) from the same generation were acquired and used for the *in vivo* PET scans. Mice underwent the following *in vivo* experiments separated by a one week interval to allow for full recovery.

In preparation for the scans, the animals were anesthetized with isoflurane (4% induction) and then maintained under anesthesia throughout the experiments while in the imaging chamber (2.5% maintenance). Animals were injected with ^{18}F-fallypride (3.4 ± 1.2 MBq) via tail vein outside the scanner and then quickly positioned inside an imaging chamber (M2M technologies) attached to the scanner bed. They received PET scans first with an Inveon dedicated PET scanner followed by CT scans with an Inveon Multimodality (MM) CT scanner (large area detector, 10 cm x 10 cm field-of-view, Siemens Medical Solutions, Knoxville, TN). The two scanners were mechanically docked to each other, which allowed sequential PET and CT scanning. An average time delay of 3.2 +/− 0.5 min was recorded between tracer injection and start of the dynamic PET scans.

The 2 hour ^{18}F-fallypride list-mode data were dynamically histogrammed in 25 frames (10 × 1min, 5 × 2 min, 10 × 1 min). All dynamic images were reconstructed using an OSEM 3D/ fast MAP algorithm (2 OSEM3D iterations, 18 MAP iterations) into 128 × 128 x 159 image arrays with a 0.77 mm pixel size and a slice thickness of 0.796 mm. Single frame images were reconstructed with Fourier rebinning of 3D data followed by OSEM 2D (16 subsets, 4 iterations, 2 EM iterations). All PET data were corrected for random events, scatter and photon attenuation. Normalization of detector responses will also be applied using a component-based method. All dynamic images were automatically corrected for radioactive decay. Quantitative calibration of PET images was performed by scanning a Ge-68 cylindrical phantom (6 cm diameter) with known activity and reconstructed under the same conditions as the mouse images. The CT scan following PET was used for attenuation and scatter correction of the PET data. CT images were also produced and were spatially transformed automatically to match the corresponding PET image immediately following their reconstruction. The CT images were acquired at a binning factor of 4 and were reconstructed using cone-beam reconstruction with a Shepp filter with cutoff at Nyquist frequency resulting in an image matrix of 480 × 480 x 632 and a voxel size of 0.206 mm.

2.6 Data Analysis

Processing of reconstructed images and data analysis were performed with PMOD software package (PMOD Technologies). All PET images were co-registered to an MRI mouse brain template (Ma et al., 2008). The CT images were resliced and manually co-registered via rigid transformations (translations and rotations) to match the template using PMOD Fusion toolbox. A head-and-hat approach was taken for co-registration using the skull and brain shape features visible in CT and MR template, respectively. The resulting rigid transformation matrix for each subject was subsequently applied to all the PET images to achieve co-registration to the MR template. 3D volumes of interest (VOIs) representing dorsal striatum (DStr), ventral striatum (VStr), substantia nigra/ventral tegmental area (SN/ VTA), hypothalamus (Hyp), and cerebellum (Cer) were drawn on the template. The VOIs on DStr and VStr consisted of spheres of 1 mm diameter placed symmetrically left and right with respect to midline (2 × 0.52 mm^3), scaled down versions of VOIs used previously for the rat brain for these structures (Constantinescu et al., 2011). The VOIs on SN\VTA and

Hyp were bilateral spheres of 0.6 mm (2 × 0.11 mm^3) and 0.8 mm (2 × 0.26 mm^3) diameter, respectively. The cerebellum VOI consisted of one sphere of 2 mm diameter (3.85 mm^3) placed centrally on the structure. The left and right values in VOIs for each structure were combined into a single VOI. All VOIs were transferred to PET images and the mean VOI activity (single frame data) or time activity curves (TACs, dynamic data) were extracted for each brain region. TACs analysis was performed using the PMOD kinetic toolbox. Binding potentials with respect to the non-displaceable compartment (BP_{ND}, Innis et al., 2007)) were computed from dynamic data. Cerebellum served as reference region. Interval tissue ratio (ITR) method (Ito et al., 1998) was used estimating BP_{ND} as

$BP_{ND}=\int_{t_S}^{t_E}(C(t)-C_{ref}(t))dt/\int_{t_S}^{t_E}C_{ref}(t)dt$ (1), where is C(t) is the activity in the region with specific activity, and $C_{ref}(t)$ the activity in the reference region (i.e. cerebellum). [$t_{S,}$ t_E] is the integration interval that includes the time of transient equilibrium and was [20, 120] min for ^{18}F-fallypride. Fractional D3R binding, f_{D3}, was estimated as $f_{D3}=BP_{ND}^{KO}/BP_{ND}^{WT}$ where BP_{ND}^{WT} and BP_{ND}^{KO} are the binding potentials of the WT and KO mice, respectively. This formula is based on the two assumptions: 1) binding to D3R and D2R are independent and 2) binding of the tracer in the D2 KO mice is entirely to D3R.

2.7. Statistical Analysis

Statistical differences between groups were determined using paired Student's t test. For PET experiments individual rats were imaged on multiple occasions after allowing for drug wash out (at least two week interval between PET experiments) so that they could serve as their own control. A p value of <0.05 was considered to indicate statistical significance.

3. Results

3.1 *In Vitro* Drug Effects

3.1.1. (*R*)-7-OH-DPAT Effects—The effect of (*R*)-7-OH-DPAT in rat brain horizontal slices exhibited a dose-dependent decrease in the binding of ^{18}F-fallypride in all regions of the brain (Fig 1A). As previously reported (Mukherjee et al., 1999), cerebellum serves as a reference region due to the minimal amount of ^{18}F-fallypride binding. At lower concentrations of (*R*)-7-OH-DPAT (1–10 nM) approx. 10% of ^{18}F-fallypride was displaced which most likely is at the D3R sites (Fig 1B,C). A greater displacement (approx. 30%) was seen at 100 nM suggesting displacement of ^{18}F-fallypride at all D3 receptor sites based on the binding affinities of (*R*)-7-OH-DPAT at D3R and D2R sites (Table 1). At a micromolar concentration, about 60% of ^{18}F-fallypride was displaced, suggesting that the effect of 7-OH-DPAT is likely occurring at both D3R and D2R, and at 10 μM concentration, the degree of ^{18}F-fallypride displacement exceeded 80% (Fig 1B). The difference between the striatum and nucleus accumbens regions was not significant. The displacement curves of ^{18}F-fallypride by (*R*)-7-OH-DPAT for the brain regions are shown in Fig 1C; the measured inhibitor concentrations (IC_{50}) were: striatum 87 nM and nucleus accumbens 56 nM.

Larger sagittal brain sections of rabbits were used to examine the effect of different concentrations of (*R*)-7-OH-DPAT on the binding of ^{18}F-fallypride in striatal and extrastriatal regions. Binding of ^{18}F-fallypride was seen in several regions in the rabbit brain as see in Fig 2A–C. High binding regions included the striatal regions (caudate and putamen), while moderate levels of binding were seen in the nucleus accumbens, olfactory tubercle and substantia nigra. These findings in the rabbit brain are generally consistent with ^{18}F-fallypride distribution in the rat brain reported previously (Mukherjee et al., 1999). The effect of (*R*)-7-OH-DPAT on ^{18}F-fallypride binding in different parts of the brain were significant. At high concentrations (10 μM) of (*R*)-7-OH-DPAT, greater than 90% of ^{18}F-fallypride was displaced from various brain regions (caudate, putamen, nucleus accumbens, olfactory tubercle and substantia nigra) as seen in Fig 2D. At lower doses of (*R*)-7-OH-DPAT approx. 15% of ^{18}F-fallypride was displaced from olfactory tubercle and nucleus accumbens regions. Similar levels of displacement of ^{18}F-fallypride by (*R*)-7-OH-DPAT occurred in the substantia nigra (Fig 2D). The displacement curves of ^{18}F-fallypride by (*R*)-7-OH-DPAT for the brain regions are shown in Fig 2E; the measured inhibitor concentrations (IC_{50}) were: caudate 81 nM, putamen 87 nM, nucleus accumbens (including olfactory tubercle) 56 nM and substantia nigra 53 nM.

3.1.2. BP 897 and NGB 2904 Effects—Rat brain sagittal slices were used to evaluate the effect of BP 897 and NGB 2904 on the binding of ^{18}F-fallypride. NGB 2904 was able to displace 40 to 50% of ^{18}F-fallypride bound to the dorsal and ventral striata. BP897, on the other hand, displaced more than 90% of ^{18}F-fallypride at 10 μM concentrations (Fig 3). In comparison, at 10 μM concentration of (*R*)-7-OH-DPAT, approx. 75% of ^{18}F-fallypride was displaced in the dorsal striatum. Extent of displacement of ^{18}F-fallypride in the dorsal and ventral striata for BP 897 and NGB 2904 were approximately similar. The displacement by (*R*)-7-OH-DPAT in the ventral striata was lower than in the dorsal striata. Thus, the rank order of the drugs for displacement of ^{18}F-fallypride was BP 897 > (*R*)-7-OH-DPAT > NGB 2904 as seen in Fig 3F.

3.2 *In Vivo* Drug Effects

3.2.1. (*R*)-7-OH-DPAT Effects—In order to evaluate the ability of (*R*)-7-OH-DPAT to compete with the binding of ^{18}F-fallypride, a dose-escalation study of (*R*)-7-OH-DPAT (from 0.015 mg/kg to 1.88 mg/kg) was carried out. After 90 minutes post-injection of ^{18}F-fallypride, a measured dose of (*R*)-7-OH-DPAT was injected intravenously. The time-activity curves for the dorsal striatum and ventral striatum are shown in Fig 4. All doses of (*R*)-7-OH-DPAT affected the binding of ^{18}F-fallypride in both the dorsal striatum and ventral striatum. The degree of ^{18}F-fallypride displacement is listed in Table 2. At the lowest dose (0.015 mg/kg), the dorsal striatum binding was reduced by 22%, while at the highest dose (1.88 mg/kg) dorsal striatum binding was reduced by 58%. A greater displacement of ^{18}F-fallypride occurred in the ventral striatum (29% and 77% respectively). In all the four doses, ventral striatum exhibited a slightly greater displacement.

3.2.2. BP 897 Effects—Upon intravenous administration of BP 897 at 90 minutes post-injection of ^{18}F-fallypride, the displacement effect of BP 897 (3 mg/kg) on ^{18}F-fallypride binding was evident in the dorsal striatum and ventral striatum (Fig 5A). BP 897 was able to displace 24–29% of ^{18}F-fallypride bound to dorsal and ventral striatum thus confirming blood brain barrier (BBB) penetration of BP 897 and interaction with the dopamine D2 and D3 receptors.

3.2.3. NGB 2904 Effects

Similar to the BP 897 experiments, intravenous administration of NGB 2904 (4 mg/kg) at 90 minutes post-injection of ^{18}F-fallypride, the displacement effect of NGB 2904 on ^{18}F-fallypride binding was not evident in the dorsal striatum and ventral striatum (Fig 5B). Based on the *in vitro* findings of NGB 2904, it was expected to compete with the binding of ^{18}F-fallypride bound to dorsal and ventral striatum. The inability of NGB 2904 to displace ^{18}F-fallypride *in vivo* may be due to poor BBB penetration. Further confirmation of the absence of the effect of NGB 2904 *in vivo* on ^{18}F-fallypride was made by a double displacement experiment. After intravenous administration of ^{18}F-fallypride, NGB 2904 was administered at 90 minutes. No effect was seen on the binding of ^{18}F-fallypride in the striata. At 150 mins, BP 897 was injected which showed an immediate displacement of ^{18}F-fallypride from the striatum.

3.3 Knock-out mice studies

PET images of ^{18}F-fallypride in the WT mouse brain revealed the expected binding pattern for this tracer with high uptake in the striatum and reduced uptake in other extrastriatal regions with concentration of D2/D3 receptors. Most notably, in the KO mouse the striatal uptake was reduced significantly. Figure 6 displays images in horizontal orientation (dorsal to ventral) of both WT and KO mouse brain normalized to the MR brain template. The relative position of each image is also provided with respect to the most dorsal section. Placement of all VOIs is shown as displayed on the MR template.

Figure 6D shows time-activity curves of ^{18}F-fallypride normalized to the injected dose in all the regions of interest, including the cerebellum from both the WT and KO mice. The ranking of ^{18}F-fallypride uptake in the WT mouse was DST > VST > Hyp > SN/VTA > Cer. In the KO mouse the tracer uptake in DStr was reduced and the clearance was fast. The uptake ranking was Hyp > SN/VTA >VST > Cer> DStr. In the WT mouse the uptake at later time points in the cerebellum were higher than in the dorsal striatum due to spill-in from skull and glands surrounding the brain.

^{18}F-Fallypride binding potentials along with the fractional D3R binding, f_{D3}, of ^{18}F-fallypride in VST, SN/VTA, and Hyp are presented in Table 3. In the WT mouse the largest BP_{ND} values were found in the DST, followed by VST, Hyp, and SN/VTA for both tracers. In the KO mice the ^{18}F-fallypride BP_{ND} values in DST were small and negative and are listed as 0. They were positive in all other regions.

4. Discussion

Because of the high affinity of ^{8}F-fallypride to both D2R and D3R receptors *in vitro* (Table 1), it is assumed that binding of ^{18}F-fallypride obtained autoradiographically or by PET, represents binding of ^{18}F-fallypride to both receptor subtypes. However, the degree to which ^{8}F-fallypride binds to these receptor subtypes in the various brain regions is not known.

A major challenge has been the lack of high selectivity drugs for D2R and D3R subtypes. It has been shown previously that 7-OH-DPAT binds to both D3R and D2R high-affinity ($D2R_{high}$) sites with K_d of 0.57/2.4 nM for D3R and K_d of 56/89 nM for $D2R_{high}$ (van Vliet et al., 1996). The binding of 7-OH-DPAT to the uncoupled D2R low-affinity ($D2_{low}$) sites was found to be too low (Gonzalez and Sibley, 1995). We have previously shown that ^{11}C-5-OH-DPAT is able to penetrate the rodent and nonhuman primate brain (Mukherjee et al., 2000). Uptake of ^{11}C-5-OH-DPAT in the rat brain was approximately 1% of the injected dose. Assuming similarity of blood brain barrier permeability and uptake between ^{11}C-5-OH-DPAT and (*R*)-7-OH-DPAT (due to their structural similarity being identical except for the position of the the phenolic hydroxyl group), we would thus be able to approximately assess the brain concentration of intravenously injected (*R*)-7-OH-DPAT. This would enable an approximate assessment of the in vivo inhibitory effects of (*R*)-7-OH-DPAT on ^{18}F-fallypride at receptor subtypes.

Thus at an intravenous dose of 0.015 mg/kg of (*R*)-7-OH-DPAT, the brain concentration of (*R*)-7-OH-DPAT may be approximated to 0.6 to 1 nM. At this concentration approximately 20% of ^{18}F-fallypride was displaced. This is consistent with our *in vitro* studies in the rat brains where approx. 20% of ^{18}F-fallypride was displaced at 1 to 10 nM concentrations of (*R*)-7-OH-DPAT. Because (*R*)-7-OH-DPAT has a >37 fold selectivity for the D3R and a K_d for D3R <3 nM (Table 1), it may be reasonable to assume that this ^{18}F-fallypride displacement/competition by (*R*)-7-OH-DPAT is at the D3R. At the higher dose of 1.88 mg/kg, which may lead up to brain concentrations of approximately 100 nM, greater than 50% of ^{18}F-fallypride was displaced which appears to be consistent with the measured *in vitro* IC_{50} of 87 nM for (*R*)-7-OH-DPAT in the striatum of rat brain slices for the displacement of ^{18}F-fallypride. This most likely includes the displacement/competition of ^{18}F-fallypride by (*R*)-7-OH-DPAT at the $D2R_{high}$ sites as well, since the reported K_d of (*R*)-7-OH-DPAT for $D2R_{high}$ is 56/89 nM (Gonzalez and Sibley, 1995; van Vliet et al., 1996). Based on the *in vitro* and *in vivo* experiments presented here with (*R*)-7-OH-DPAT, up to 75–80% of the total amount of ^{18}F-fallypride was displaced at approximately 100 nM (*R*)-7-OH-DPAT. In experiments with ^{125}I-epidepride, 100 nM of (*R*)-7-OH-DPAT was used to assess degree of D3R displacement (Gurevich and Joyce, 1999).. The (*R*)-7-OH-DPAT induced nondisplaceable component of ^{18}F-fallypride is likely to be the $D2R_{low}$ sites since (*R*)-7-OH-DPAT has weak affinity at $D2R_{low}$.

Effect of (*R*)-7-OH-DPAT on rabbit brain slices did not significantly differentiate between the brain regions. The substantia nigra, nucleus accumbens and olfactory tubercle that were clearly delineated in the rabbit brains were similarly affected by (*R*)-7-OH-DPAT. The measured IC_{50} for substantia nigra and nucleus accumbens were 53 nM and 56 nM, respectively, which are slightly better than that measured for caudate and putamen, perhaps suggestive of a D3R component. However, it must be noted that a clear regional brain distribution of D3R was not evident in the four brain regions (caudate, putamen, nucleus accumbens and substantia nigra). Extent of competition by (*R*)-7-OH-DPAT of ^{18}F-fallypride was similar in these regions, however, subtle differences cannot be ruled out.

The D3R selective drugs (>50-fold selective for D3R over D2R), BP 897, a partial agonist and NGB 2904, an antagonist were both able to compete with ^{18}F-fallypride *in vitro* in rat brain slices. The competition by BP 897 was greater than NGB 2904, and neither of them exhibited significant difference between dorsal and ventral striatum, although it must be noted that only a single concentration of 10 μM was used in order to demonstrate competition of these drugs with ^{18}F-fallypride in vitro. In vivo however, NGB 2904 was not able to displace ^{18}F-fallypride in the striatum. Although NGB 2904 is being used for animal model studies (e.g., Banasikowski and Beninger, 2012), our findings suggest that it may have poor brain penetration. On the other hand, BP 897 had a significant measureable effect on ^{18}F-fallypride displacing >20% which may be attributed to D3R, although some D2R cannot be ruled out. Thus, although competition/displacement studies with D3R selective drugs proved to be useful, interpretation still is a challenge due to mixed effects on both receptor subtypes.

Use of D2R knock-out mice has thus been carried out in an attempt to avoid the receptor overlap. The D3R binding fractions relative to the total D2R/D3R of ^{18}F-fallypride in different regions of the mouse brain were computed. Binding potentials in the dorsal striatum of WT mice for ^{18}F-fallypride scanned at baseline were about 40% lower than those reported (Rominger et al., 2010) from *in vivo* microPET with saline pre-injection and using Logan non-invasive for computation with similar scan time intervals (0–120 min for ^{18}F-fallypride). These differences are likely due to the differences in the impact of both partial volume effect and spillover activity between the two studies. Another cause for discrepancy could come from different methods for computation of binding potentials being used (Logan non-invasive versus interval tissue ratios, voxel- versus VOI-based analysis). As expected, ^{18}F-fallypride binding potentials in the dorsal striatum of the WT mice were higher than in the ventral striatum and other extrastriatal regions. D2 KO mice lacked binding of ^{18}F-fallypride in dorsal striatum indicating the absence of D2R in KO mice. Low but detectable binding of ^{18}F-fallypride in VST, SN/VTA and Hyp that could be in part attributed to D3R which was observed and estimated in the WT mouse.

By comparing the KO and WT binding at baseline we computed the fraction of ^{18}F-fallypride to D3R relative to D2R and D3R combined. The fraction D3R (f_{D3}) calculations were made based on two assumptions. First, it was assumed that the WT and D2 KO mice had the same amount of receptor density in all regions and, second, that the variability of ^{18}F-fallypride binding was low compared with the differences between WT and KO. From these calculations the largest D3 fractions were found in SN/VTA and hypothalamus (~100%) suggesting that binding sites in these structures consist mostly of D3R. These findings are supported by a previous study using autoradiography in mice that showed high ^{11}C-(+)-PHNO binding in these two regions (Rabiner et al., 2009). The D3R binding fraction of ^{18}F-fallypride in ventral striatum was 15%. Although these values are similar to those computed for ^{11}C-PHNO in human brain (100% for substantia nigra and hypothalamus, 26% for ventral striatum) (Tziortzi et al., 2011), the lack of ^{18}F-fallypride binding in the dorsal striatum is not consistent with recent results with partial agonist ^{3}H-LS-3–134 (Rangel-Barajas et al., 2014) (Table 4). Because of the potential complexities associated with knock-out mice (Eisener-Dorman et al., 2009), additional studies are needed with the KO mice in order to confirm the *in vivo* findings.

There are two major limiting factors that impacted the quantification of mouse images and which need to be taken in account: spillover effects and partial volume effects (PVEs). The first factor consists of a slowly increasing spillover signal from outside the brain (skull and glands) due to free tracer and defluorination, into adjacent brain structures of interest. This can be noted from examination of the time-activity curves of ^{18}F-fallypride presented in Fig. 6D,E. The activity cleared faster from DST than from all the other regions, including the cerebellum. Curves from cerebellum, SN\VTA, VST and Hyp remained constant or even showed a slow increase at late time points due to the spillover contribution surpassing the tracer washout. Apart from kinetic differences among regions this can be attributed to the different degrees in which the spillover activity from glands and skull contribute to the activity in all regions over time. DST is minimally contaminated by the skull and glands activity due to its deep location inside the brain and away from the skull. We did not employ any methodology aimed to correct for the spillover effects but in order to reduce them shorter integration intervals were chosen for computation of BP_{ND}s. the cerebellar reference region was placed centrally instead of on the cerebellar lobes. On a side note, evidence from studies with ^{11}C-PHNO point to a minimal presence of the D3R localized in cerebellar lobes 9 and 10 (Rabiner et al., 2009). Spillover correction methods such as the one proposed by Millet et al. for the rat brain using factor analysis may be implemented to future mouse studies (Millet et al., 2012).

Since the mouse brain structures are small with respect to the resolution of our scanner (~1.47 mm, (Constantinescu and Mukherjee, 2009) partial volume effects (PVEs) were significant, which means that the observed accumulated activity in these structures was most likely underestimated. BP_{ND} estimates were impacted by the PVE because the recovery coefficients for the target and reference region are different.

Evidence of D3 Receptors using imaging methods

Since the discovery and characterization of the D3R (Sokoloff et al., 1990), several reports using immunohistochemistry have confirmed the presence of D3R in rodent brains. For example, signifcant D3R mRNA has been measured in the islands of Calleja and smaller amounts in nucleus accumbens (Guo et al., 1998). Immunostaining confirmed the presence of D3R in several brain regions including islands of Calleja (Diaz 2000). *In vitro* autoradiographic methods have been used to ascertain the distribution of the D3R by several different radioligands. Several studies were reported using ^{3}H-7-OH-DPAT for localization to D3R, but was subsequently also found to bind to $D2_{high}$ receptor sites (Gonzalez and Sibley, 1995). ^{11}C-PHNO is a modified aminotetralin derivative and has high affinity for $D2R_{high}$ and D3R receptor subtypes thus suggesting that PHNO binds to $D2R_{high}$ and D3R, both *in vitro* and *in vivo*. PET imaging studies indicate differences in binding pattern in animals as well as humans when compared to raclopride. Along with binding to the caudate-putamen, binding appears to be greater in the globus pallidus indicating a possible D3R–preferred binding (Seeman et al., 2006; Searle et al., 2010). A close analog, ^{125}I-7-OH-PIPAT has been used for autoradiographic studies with binding seen in the islands of Calleja, nucleus accumbens and least in the striatum (Mugnani et al., 2013). An early study used ^{3}H-PD 128907, a close analog of PHNO, included brain sections from mouse, rat, guinea pig and rabbit and confirmed presence of binding sites in several brain regions with maximal levels of binding in the islands of Calleja, followed by anteroventral caudate and nucleus accumbens (Levant 1998). Like PHNO, ^{3}H-PD128907 is likely a D3R preferred radioligand with a high liklihood of binding to D2$_{high}$ sites as well. Similarly, we have reported ^{11}C-5-OH-DPAT and ^{18}F-5-OH-FPPAT, which bind to striatum *in vitro* and *in vivo* and are sensitive to Gpp(NH)p and are considered as D2R$_{high}$ binding agents (Mukherjee et al., 2000; Shi et al., 2004). The D3R component of these derivatives have yet to be determined. In an effort to make the derivatives D3R preferring, we are currently evaluating ^{18}F-7-OH-FHXPAT (Majji et al., 2010). Several phenylpiperazine derivatives have been developed as partial agonists for the D3R (Mach et al., 2011). Using one such derivative, ^{3}H-LS-3–134, both nucleus accumbens and striatum were found to contain D3R, with the former having two-fold more receptors (Rangel-Barajas et al., 2014). Comparative studies with the agonist ^{3}H-PHNO and ^{3}H-raclopride indicate an absence of binding of ^{3}H-raclopride in the cerebellum lobules 9 and 10, suggestive of a lack of D3R binding of raclopride compared to PHNO (Kiss et al., 2011). Thus, it appears that there are sufficient D3R in the brain that make *in vivo* imaging a viable approach to study their role in brain function. However, regional localization and concentration of D3R remains to be further verified by selective radioligands.

In this work, using fallypride, we were able to surmise that the predominant binding of ^{18}F-fallypride both *in vitro* and *in vivo* was to D2R$_{high}$. ^{18}F-Fallypride binding to dopamine D3R was evidenced by its displacement by selective dopamine D3R ligands at low doses *in vivo* and the residual binding in D2R KO mice. Binding to D3R was low, and based on our *in vitro* and *in vivo* experiments it is likely to be 20% (Fig 7). This level of D3R appears to be consistent with human postmortem D3R levels reported in caudate-putamen (Gurevich and Joyce, 1999). Cofirmation of this D3R level of ^{18}F-fallypride binding and regional brain variations in vivo will need further work.

Limitations of the Study

Differentiation of extent of binding of ^{18}F-fallypride to D3R and D2R by using selective drugs is a challenge. Even though the drugs used have selectivities of >50 fold for D3R, they do not exclusively effect D3R but also compete at the D2R. More selective D3R and D2R drugs may offer additional supporting information. The knock-out mice offer an alternative to study in vivo selectivity, but technical issues of imaging small brain regions and paradoxical aspects of knock-out models can be difficult to interpret. Species differences in the levels of D3R across brain regions also may be expected which has not been addressed here. The measurements reported here are based on extent of displacement of ^{18}F-fallypride and are therefore not quantitative with respect to the concentration of D3R.

Conclusion

^{18}F-Fallypride binds to dopamine D3R as evidenced by its competition/displacement by selective dopamine D3R ligands. Up to 20% of ^{18}F-fallypride may be bound to D3R *in vivo*, but this will require further verification by using more selective drugs for D2R and D3R. Differences in brain regional distribution of D3R binding of ^{18}F-fallypride will require further studies. The D3R antagonist, NGB 2904 showed significant competition with ^{18}F-fallypride *in vitro*, but did not displace ^{18}F-fallypride *in vivo*.

Acknowledgements

This research study was supported by National Institute of Health grants NIH DA038886 (JM) and NIH EB006110 (JM). We like to thank Dr. Emiliana Borrelli for the D2R knock-out mice. Technical assistance of Evegeni Sevrioukov is acknowledged.

References

Baba S, Enomoto T, Horisawa T, Hashimoto T, Ono M. Blonanserin extensively occupies rat dopamine D3 receptors at antipsychotic dose range. J Pharm Sci. 2015; 127:326–331.

Baik JH, Picetti R, Saiardi A, Thiriet G, Dierich A, Depaulis A, Le Meur M, Borrelli E. Parkinsonian-like locomotor impairment in mice lacking dopamine D2 receptors. Nature. 1995; 377:424–428. [PubMed: 7566118]

Banasikowski TJ, Beninger RJ. Reduced expression of haloperidol conditioned catalepsy in rats by the dopamine D3 receptor antagonists nafadotride and NGB 2904. Eur Neuropsychopharmacol. 2012; 22:761–768. [PubMed: 22410316]

Boulay D, Depoortere R, Perrault Gh, Borrelli E, Sanger DJ. Dopamine D2 receptor knock-out mice are insensitive to the hypolocomoter and hypothermic effects of dopamine D2/D3 receptor agonists. Neuropharmacology. 1999; 38:1389–1396. [PubMed: 10471093]

Christian BT, Vandehey NT, Fox AS, Murali D, Oakes TR, Converse AK, Nickles RJ, Shelton SE, Davidson RJ, Kalin NH. The distribution of D2/D3 receptor binding in the adolescent rhesus monkey using small animal PET imaging. Neuroimage. 2009; 44:1334–1344. [PubMed: 19015034]

Constantinescu CC, Mukherjee J. Performance evaluation of an Inveon PET preclinical scanner. Phys Med Biol. 2009; 54:2885–2899. [PubMed: 19384008]

Constantinescu CC, Coleman RA, Pan ML, Mukherjee J. Striatal and extrastriatal microPET imaging of D2/D3 dopamine receptors in rat brain with [(18)F]fallypride and [(18)F]desmethoxyfallypride. Synapse. 2011; 65:778–787. [PubMed: 21218455]

Davoodi N, te Riele P, Langlois X. Examining dopamine D3 receptor occupancy by antipsychotic drugs via [3H]7-OH-DPAT ex vivo autoradiography and its cross-validation via c-fos immunohistochemistry in the rat brain. Eur. J. Pharmacol. 2014; 740:669–675. [PubMed: 24967534]

Diaz J, Pilon C, LeFoll B, Gros C, Triller A, Schwartz J-C, Sokoloff P. Dopamine D3 receptors expressed by all mesencephalic neurons. J. Neuroscience. 2000; 20:8677–8684. [PubMed: 11102473]

Everitt BJ, Wolf ME. Psychomotor stimulant addiction: a neural systems perspective. J Neurosci. 2002; 22:3312–3320. [PubMed: 11978805]

Everitt BJ, Robbins TW. Neural systems of reinforcement for drug addiction: from actions to habits to compulsion. Nat Neurosci. 2005; 8:1481–1489. [PubMed: 16251991]

Gallezot JD, Beaver JD, Gunn RN, Nabulsi N, Weinzimmer D, Singhal T, et al. Affinity and selectivity of [(1)(1)C]-(+)-PHNO for the D3 and D2 receptors in the rhesus monkey brain in vivo. Synapse. 2012; 66:489–500. [PubMed: 22213512]

Gilbert JG, Newman AH, Gardner EL, Ashby CR Jr, Heiderberger CA, Pak AC, Peng XQ, Xi ZX. Acute administration of SB-277011A, NGB 2904, or BP 897 inhibits cocaine cue-induced reinstatement of drug-seeking behavior in rats: role of dopamine D3 receptors. Synapse. 2005; 57:17–28. [PubMed: 15858839]

Ginovart N, Galineau L, Willeit M, Mizrahi R, Bloomfield PM, Seeman P, Houle S, Kapur S, Wilson AA. Binding characteristics and sensitivity to endogenous dopamine of [11C]-(+)-PHNO, a new agonist radiotracer for imaging the high-affinity state of D2 receptors in vivo using positron emission tomography. J Neurochem. 2006; 97:1089–1103. [PubMed: 16606355]

Gonzalez AM, Sibley DR. 3H–OH-DPAT is capable of labeling dopamine D2 as well as D3 receptors. Eur J Pharmacol. 1995; 272:R1–R3. [PubMed: 7713138]

Graff-Guerrero A, Willeit M, Ginovart N, Mamo D, Mizrahi R, Rusjan P, et al. Brain region binding of the D2/3 agonist [11C]-(+)-PHNO and the D2/3 antagonist [11C]raclopride in healthy humans. Hum Brain Mapp. 2008; 29:400–410. [PubMed: 17497628]

Author Manuscript

Author Manuscript

Author Manuscript

Graff-Guerrero A, Redden L, Abi-Saab W, Katz DA, Houle S, Barsoum P, et al. Blockade of [11C](+)-PHNO binding in human subjects by the dopamine D3 receptor antagonist ABT-925. Int J Neuropsychopharmacol. 2010; 13:273–287. [PubMed: 19751545]

Guo N, Vincent SR, Fibiger HC. Phenotypic characterization of neuroleptic-sensitive neurons in the forebrain: contrasting targets of haloperidol and clozapine. Neuropsychopharmacology. 1998; 18:133–145. [PubMed: 9629567]

Gurevich EV, Joyce JN. Distribution of dopamine D3 receptor expressing neurons in the human forebrain: Comparison with D2 receptor expressing neurons. Neuropsychopharm. 1999; 20:60–80.

Heidbreder CA, Gardner EL, Xi ZX, Thanos PK, Mugnaini M, Hagan JJ, et al. The role of central dopamine D3 receptors in drug addiction: a review of pharmacological evidence. Brain Res Brain Res Rev. 2005; 49:77–105. [PubMed: 15960988]

Heidbreder CA, Newman AH. Current perspectives on selective dopamine D(3) receptor antagonists as pharmacotherapeutics for addictions and related disorders. Ann N Y Acad Sci. 2010; 1187:4–34. [PubMed: 20201845]

Eisener-Dorman AF, Lawrence DA, Bolivar VJ. Cautionary insights on knockout mouse studies: The gene or not the gene. Brain Behav Immuno. 2009; 23:318–324.

Innis RB, Cunningham VJ, Delforge J, Fujita M, Gjedde A, Gunn R, Holden J, Huang SC, Ichise M, Iida H, Ito H, Kimura Y, Koeppe RA, Knudsen GM, Knuuti J, Lammertsma AA<Laruelle M, Logan J, Maguire RP, Mintun MA, Morris ED, Parsey R, Price JC, Slifstein M, Sossi V, Suhara T, Votaw JR, Wong DF, Carson RE. Consensus nomenclature for in vivo imaging of reversibly-binding radioligands. J Cereb Blood Flow Metab. 2007:1533–1539. [PubMed: 17519979]

Ito H, Hietala J, Blomqvist G, Halldin C, Farde L. Comparison of the transient equilibrium and continuous infusion method for quantitative PET analysis of [11C]raclopride binding. J Cereb Blood Flow Metab. 1998; 18:941–950. [PubMed: 9740097]

Kiss B, Horti F, Bobok A. In vitro and in vivo comparison of $[^3H]$(+)-PHNO and $[^3H]$raclopride binding to rat striatum and lobes 9 and 10 of the cerebellum: a method to distinguish dopamine D3 from D2 receptor sites. Synapse. 2011; 65:467–478. [PubMed: 20936685]

Koob GF, Le MM. Drug abuse: hedonic homeostatic dysregulation. Science. 1997; 278:52–58. [PubMed: 9311926]

Le Foll B, Wilson AA, Graff A, Boileau I, Di Ciano P. Recent methods for measuring dopamine D3 receptor occupancy in vivo: importance for drug development. Frontiers Pharmacology. 2014; 5:1–12.

Lejeune F, Newman-Tancredi A, Audinot V, Millan MJ. Interactions of (+)- and (−)-8- and 7-hydroxy-2-(di-n-propylamino)tetralin at human (h)D3, hD2 and h serotonin 1A receptors and their modulation of the activity of serotonergic and dopaminergic neurons in rats. J. Pharmacol. Exp. Ther. 1997; 280:1241–1249. [PubMed: 9067310]

Levant B. Differential distribution of D3 dopamine receptors in the brains of mammalian species. Brain Research. 1998; 800:269–274. [PubMed: 9685676]

Loiseau F, Millan MJ. Blockade of dopamine D(3) receptors in frontal cortex, but not in sub-cortical structures, enhances social recognition in rats: similar actions of D(1) receptor agonists, but not of D(2) antagonists. Eur Neuropsychopharmacol. 2009; 19:23–33. [PubMed: 18793829]

Ma Y, Smith D, Hof PR, Foerster B, Hamilton S, Blackband SJ, Yu M, Benveniste M. In Vivo 3D Digital Atlas Database of the Adult C57BL/6J Mouse Brain by Magnetic Resonance Microscopy. Front Neuroanat. 2008; 2:1. [PubMed: 18958199]

Mach RH, Tu Z, Xu J, Li S, Jones LA, Taylor M, Luedtke RR, Derdeyn CP, Perlmutter JS, Mintun MA. Endogenous dopamine (DA) competes with the binding of a radiolabeled D receptor partial agonist in vivo: a positron emission tomography study. Synapse. 2011; 65:724–732. [PubMed: 21132811]

Majji D, Pan ML, Mirbolooki RM, Constantinescu C, Mukherjee J. Rodent PET evaluation of fluorine-18 labeled dopamine D3 receptor agonist, 18F-7-OH-FHXPAT. J. Nucl. Med. 2012; 53(suppl):1634.

Malmberg A, Nordvall G, Johansson AM, Mohell N, Hacksell U. Molecular basis for the binding of 2-aminotetralins to human dopamine D2A and D3 receptors. Mol. Pharmacol. 1994; 46:299–312. [PubMed: 8078492]

McCormick PN, Wilson VS, Wilson AA, Remington GJ. Acutely administered antipsychotic drugs are highly selective for dopamine D2 over D3 receptors. Pharmacol Res. 2013; 70:66–71. [PubMed: 23327779]

McFarland K, Kalivas PW. The circuitry mediating cocaine-induced reinstatement of drug-seeking behavior. J Neurosci 2001. 2001; 21:8655–8663.

McFarland K, Davidge SB, Lapish CC, Kalivas PW. Limbic and motor circuitry underlying footshock-induced reinstatement of cocaine-seeking behavior. J Neurosci. 2004; 24:1551–1560. [PubMed: 14973230]

Millet P, Moulin-Sallanon M, Tournier BB, Dumas N, Charnay Y, Ibanez V. Quantification of dopamine D(2/3) receptors in rat brain using factor analysis corrected [(18)F]Fallypride images. Neuroimage. 2012; 62:1455–1468. [PubMed: 22659483]

Mugnani M, Iavarone L, Cavallini P, Griffante C, Oliosi B, Savoia C, Beaver J, Rabiner EA, Micheli F, Heidbreder C, Andorn A, Pich EM, Bani M. Occupancy of brain dopamine D3 receptors and drug craving: A translational approach. Neuropsychopharm. 2013; 38:302–313.

Mukherjee J, Christian BT, Dunigan KA, Shi B, Narayanan TK, Satter M, Mantil J. Brain imaging of 18F–fallypride in normal volunteers: blood analysis, distribution, test-retest studies, and preliminary assessment of sensitivity to aging effects on dopamine D-2/D-3 receptors. Synapse. 2002; 46:170–188. [PubMed: 12325044]

Mukherjee J, Narayanan TK, Christian BT, Shi B, Dunigan KA, Mantil J. In vitro and in vivo evaluation of the binding of the dopamine D2 receptor agonist 11C-(R,S)-5-hydroxy-2-(di-n-propylamino)tetralin in rodents and nonhuman primate. Synapse. 2000; 37:64–70. [PubMed: 10842352]

Mukherjee J, Yang ZY, Brown T, Wernick M, Yasillo NJ, Ouyang X, Chen C-T, Mintzer R, Cooper M. Preliminary assessment of extrastriatal dopamine D-2 receptor binding in the rodent and non-human primate brains using the high affinity radioligand, [F-18]fallypride. Nucl Med Biol. 1999; 26:519–527. [PubMed: 10473190]

Mukherjee J, Yang ZY, Das MK, Brown T. Fluorinated benzamide neuroleptics--III. Development of (S)-N-[(1-allyl-2-pyrrolidinyl)methyl]-5-(3-[18F]fluoropropyl)-2, 3-dimethoxybenzamide as an improved dopamine D-2 receptor tracer. Nucl Med Biol. 1995; 22:283–296. [PubMed: 7627142]

Narendran R, Slifstein M, Guillin O, Hwang Y, Hwang DR, Scher E, Reeder S, Rabiner E, Laruelle M. Dopamine (D2/3) receptor agonist positron emission tomography radiotracer [11C]-(+)-PHNO is a D3 receptor preferring agonist in vivo. Synapse. 2006; 60:485–495. [PubMed: 16952157]

Paterson NE, Vocci F, Sevak RJ, Wagreich E, London ED. Dopamine D3 receptors as a therapeutic target for methamphetamine dependence. Amer J Drug Alcohol Abuse. 2014; 40:1–9. [PubMed: 24359505]

Paxinos, G.; Watson, C. The rat brain in stereotaxic coordinates. 4th Edition. San Diego, California: Academic Press; 1998.

Rabiner EA, Slifstein M, Nobrega J, Plisson C, Huiban M, Raymond R, Diwan M, Wilson AA, McCormick P, Gentile G, Gunn RN, Laruelle MA. In vivo quantification of regional dopamine-D3 receptor binding potential of (+)-PHNO: Studies in non-human primates and transgenic mice. Synapse. 2009; 63:782–793. [PubMed: 19489048]

Rominger A, Wagner E, Mille E, Boning G, Esmaeilzadeh M, Wangler B, Gildehaus FJ, Nowak S, Bruche A, Tatsch K, Bartenstein P, Cumming P. Endogenous competition against binding of [(18)F]DMFP and [(18)F]fallypride to dopamine D(2/3) receptors in brain of living mouse. Synapse. 2010; 64:313–322. [PubMed: 19957365]

Rangel-Barajas C, Malik M, Taylor M, Neve KA, Mach RH, Luedtke RR. Characterization of ^{3}H-LS-3–134, a novel arylamide phenylpiperazine D3 dopamine receptor selective radioligand. J Neurochem. 2014; 131:418–431. [PubMed: 25041389]

Searle G, Beaver JD, Comley RA, Bani M, Tziorti A, Slifstein M, Mugnaini M, Griffante C, Wilson AA, Merlo-Pich E, Houle S, Gunn R, Rabiner EA, Laruelle M. Imaging dopamine D3 receptors in the human brain with positron emission tomography, [11C]PHNO, and a selective D3 receptor antagonist. Biol Psych. 2010; 68:392–399.

Seeman P, Wilson A, Gmeiner P, Kapur S. Dopamine D2 and D3 receptors in human putamen, caudate nucleus, and globus pallidus. Synapse. 2006; 60:205–211. [PubMed: 16739118]

Shaham Y, Shalev U, Lu L, De WH, Stewart J. The reinstatement model of drug relapse: history, methodology and major findings. Psychopharmacology (Berl). 2003; 168:3–20. [PubMed: 12402102]

Shi B, Narayanan TK, Christian BT, Chattopadhyay S, Mukherjee J. Synthesis and in vitro evaluation of the binding of the dopamine D-2 receptor agonist, (*R,S*)-2-(*N*-propyl-*N*-(5-^{18}F-fluoropentyl)-5-hydroxyaminotetralin (^{18}F-5-OH-FPPAT) in rodents. Nucl Med Biol. 2004; 31:303–311. [PubMed: 15028242]

Slifstein M, Hwang DR, Huang Y, Guo N, Sudo Y, Narendran R, Talbot P, Laruelle M. In vivo affinity of [18F]fallypride for striatal and extrastriatal dopamine D2 receptors in nonhuman primates. Psychopharmacology (Berl). 2004; 175:274–286. [PubMed: 15024551]

Sokoloff P, Giros B, Martres MP, Bouthenet ML, Schwartz JC. Molecular cloning and characterization of a novel dopamine receptor (D3) as a target for neuroleptics. Nature. 1990; 347:146–151. [PubMed: 1975644]

Stark D, Piel M, Hubner H, Gmeiner P, Grunder G, Rosch F. In vitro affinities of various halogenated benzamide derivatives as potential radioligands for non-invasive quantification of D(2)-like dopamine receptors. Bioorg Med Chem. 2007; 15:6819–6829. [PubMed: 17765546]

Tantawy MN, Jones CK, Baldwin RM, Ansari MS, Conn PJ, Kessler RM, Peterson TE. [(18)F]Fallypride dopamine D2 receptor studies using delayed microPET scans and a modified Logan plot. Nucl Med Biol. 2009; 36:931–940. [PubMed: 19875049]

Tziortzi AC, Searle GE, Tzimopoulou S, Salinas C, Beaver JD, Jenkinson M, Laruelle M, Rabiner EA, Gunn RN. Imaging dopamine receptors in humans with [11C]-(+)-PHNO: dissection of D3 signal and anatomy. Neuroimage. 2011; 54:264–277. [PubMed: 20600980]

van Vliet LA, Tepper PG, Dijkstra D, Damsma G, Wikstrom H, Pugsley TA, Akunne HC, Heffner TG, Glase SA, Wise LD. Affinity for dopamine D2, D3, and D4 receptors of 2-aminotetralins. Relevance of D2 agonist binding for determination of receptor subtype selectivity. J Med Chem. 1996; 39:4233–4237. [PubMed: 8863800]

Vuckovic MG, Li Q, Fisher B, Nacca A, Leahy RM, Walsh JP, Mukherjee J, Jakowec MW, Petzinger GM. High intensity treadmill exercise upregulates striatal dopamine D2 receptor in 1-methyl-4-phenyl-1,2,3,6-tetrahydropyridine-lesioned mice: in vivo PET-imaging with ^{18}F-fallypride. Movement Disorders. 2010; 25:2777–2784. [PubMed: 20960487]

Willeit M, Ginovart N, Kapur S, Houle S, Hussey D, Seeman P, Wilson AA. High-affinity states of human brain dopamine D2/D3 receptors imaged by the agonist [11C]-(+)-PHNO. Biol. Psychiatry. 2006; 159:389–394.

Xi ZX, Li X, Li J, Peng XQ, Song R, Gaal J, Gardner EL. Blockade of dopamine D3 receptors in the nucleus accumbens and central amygdala inhibits incubation of cocaine craving in rats. Addict Biol. 2013; 18:665–677. [PubMed: 22913325]

Xi Z-X, Gilbert J, Campos AC, Kline N, Ashby CR, Hagan JJ, Heidbreder CA, Gardner EL. Blockade of mesolimbic dopamine D3 receptors inhibits stress-induced reinstatement of cocaine-seeking in rats. Psychopharmacology. 2004; 176:57–65. [PubMed: 15083257]

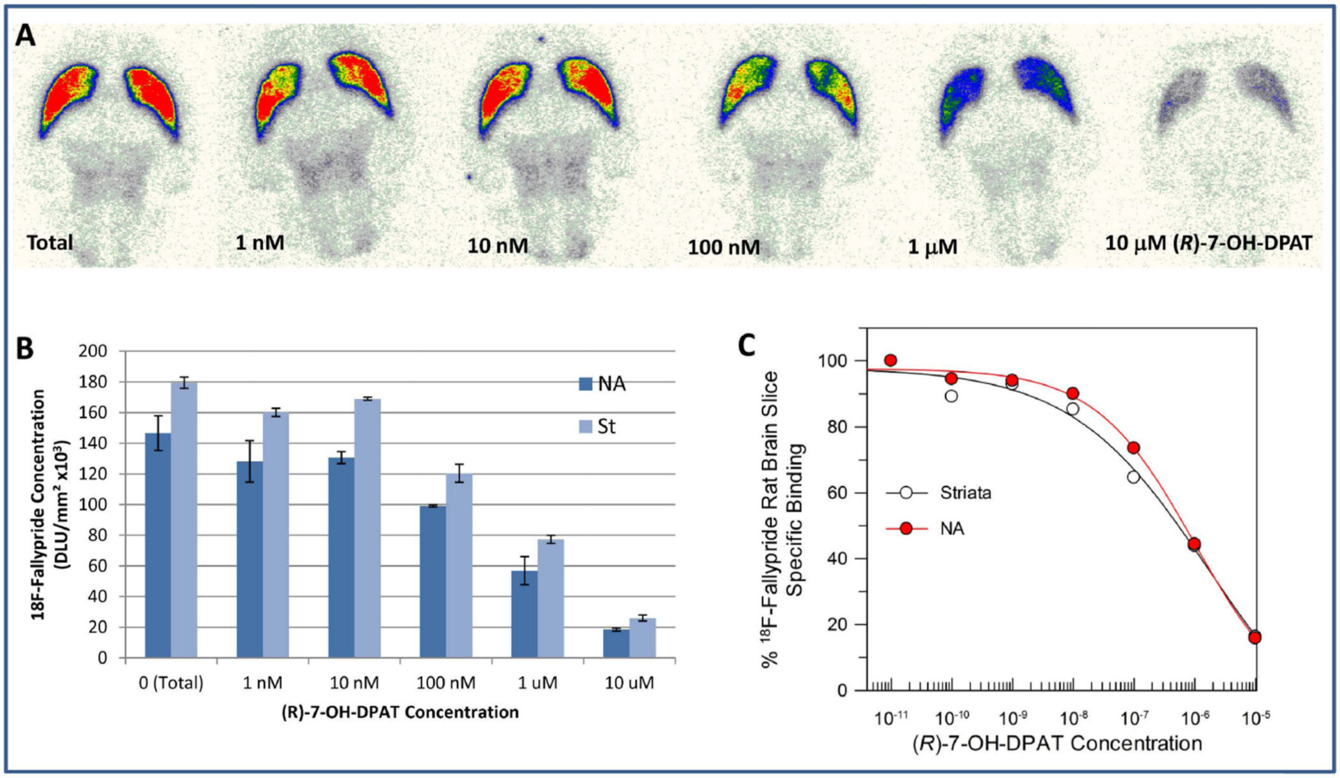

Figure 1.

(A) *In vitro* Effect of (R)-7-OH-DPAT at different concentrations (from left to right: total, 1 nM, 10 nM, 100nM, 1 μM, 10 μM) on ^{18}F-fallypride binding in ventral striatum and nucleus accumbens in rat brain; (B) Comparing ^{18}F-fallypride binding values at different concentrations of (*R*)-7-OH-DPAT; (C) Percent displacement of ^{18}F-fallypride by different concentrations of (*R*)-7-OH-DPAT.

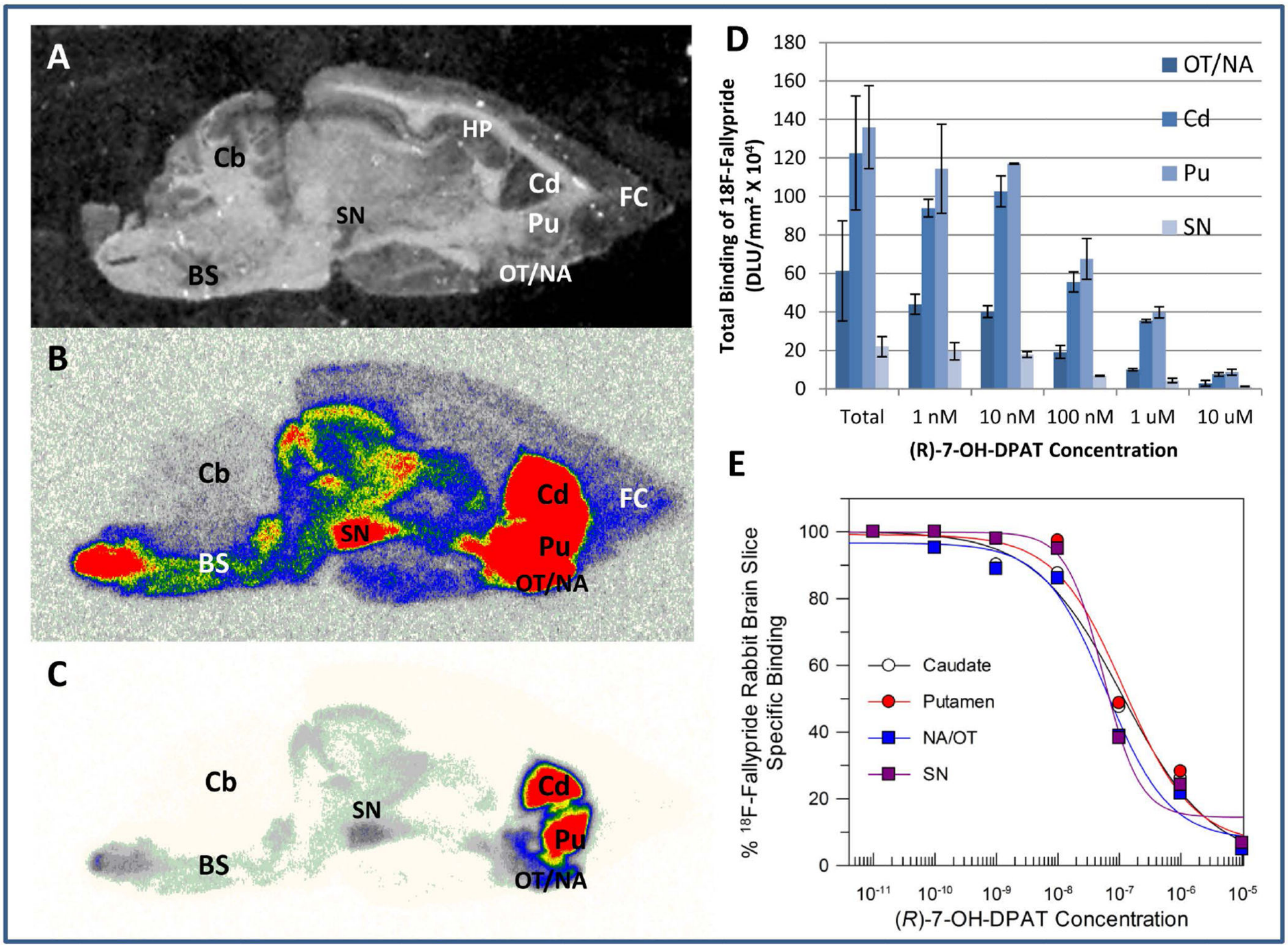

Figure 2.

(A) Sagittal rabbit brain slice; (B–C) ^{18}F-Fallypride binding in striatal and extrastriatal regions (shown at different maximum thresholds of 700 (B) and 7000 (C) DLU/mm^2, respectively; FC= frontal cortex; Cd= caudate; Pu= putamen; OT= olfactory tubercle; NA= nucleus accumbens; SN= substantia nigra; BS= brain stem; Cb= cerebellum); (D) Binding values of ^{18}F-fallypride at different concentrations of (*R*)-7-OH-DPAT; (E) Percent displacement of specifically bound ^{18}F-fallypride by (*R*)-7-OH-DPAT at different concentrations in different rabbit brain regions.

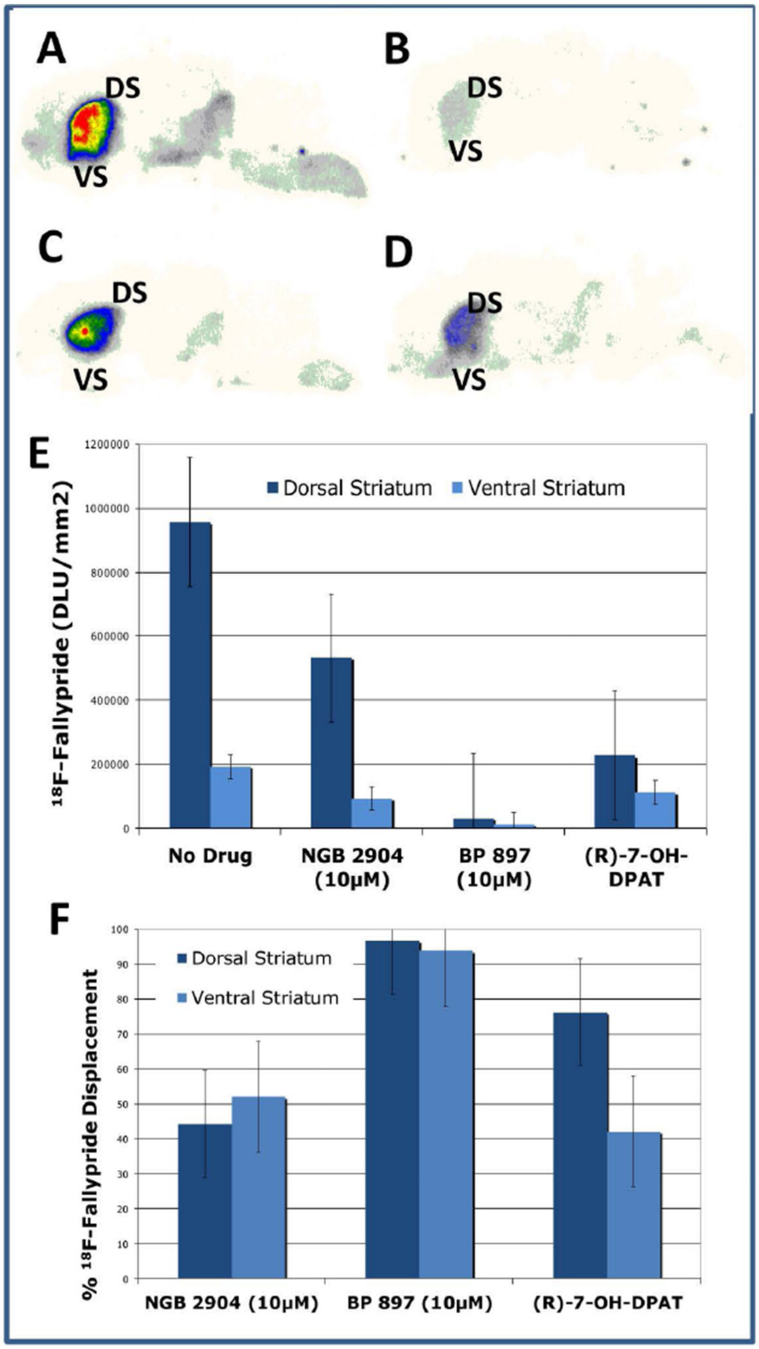

Figure 3.

In vitro ^{18}F-fallypride in rat sagittal brain slice (A) Total binding; (B) With 10μM BP 897; (C) With 10 μM NGB 2904; (D) With 10 μM (*R*)-7-OH-DPAT. DS: dorsal striatum; VS: ventral striatum. (E) ^{18}F-fallypride *in vitro* relative binding in presence of 10μM concentrations of NGB 2904, BP 897, and (*R*)-7-OH-DPAT, "No Drug" bars are representative of total ^{18}F-fallypride in the DS and VS. (F) Percent displacement of ^{18}F-fallypride by 10μM concentrations of NGB 2904, BP 897, and (*R*)-7-OH-DPAT from total binding *in vitro*, NGB 2904 is the only drug to show a higher displacement of ^{18}F-fallypride in the ventral striatum.

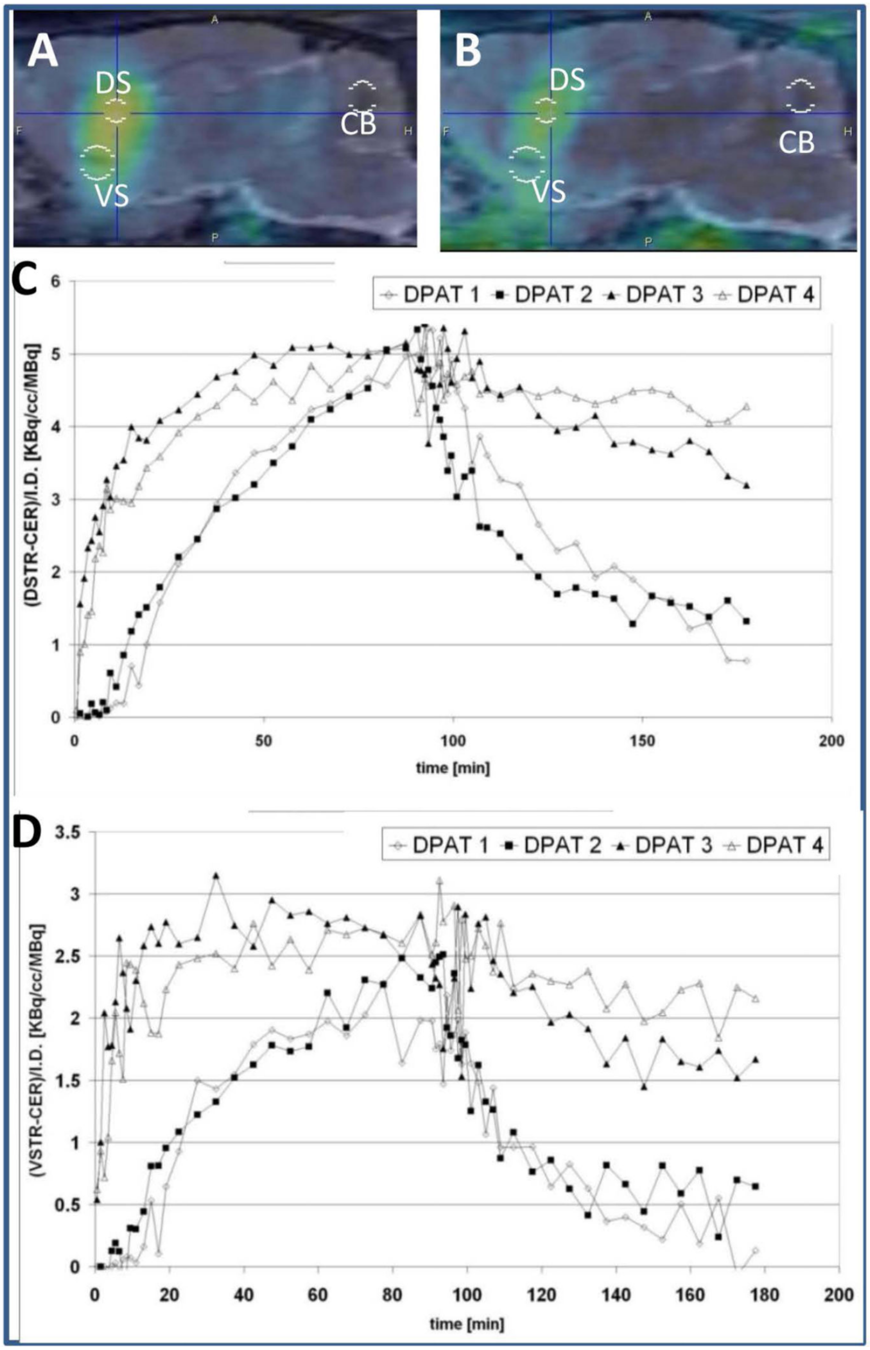

Figure 4.

(A) PET image of ^{18}F-fallypride labeled rat brain showing striatal regions from 60–90 min into scan (before administration of (*R*)-7-OH-DPAT); (B) 120–150 min into scan (postinjection of 1mg/ml (*R*)-7-OH-DPAT). DS: dorsal striatum; VS: ventral striatum; Ce: cerebellum; (C, D). Time-activity curves of ^{18}F-fallypride binding in the dorsal striatum DSTR (C) and ventral striatum VSTR (D) including displacement by different doses of (*R*)-7-OH-DPAT: 1.88mg/kg (DPAT1), 0.38 mg/kg (DPAT2), 0.06mg/kg DPAT3), 0.015mg/kg (DPAT4), administered at 90 mins postinjection.

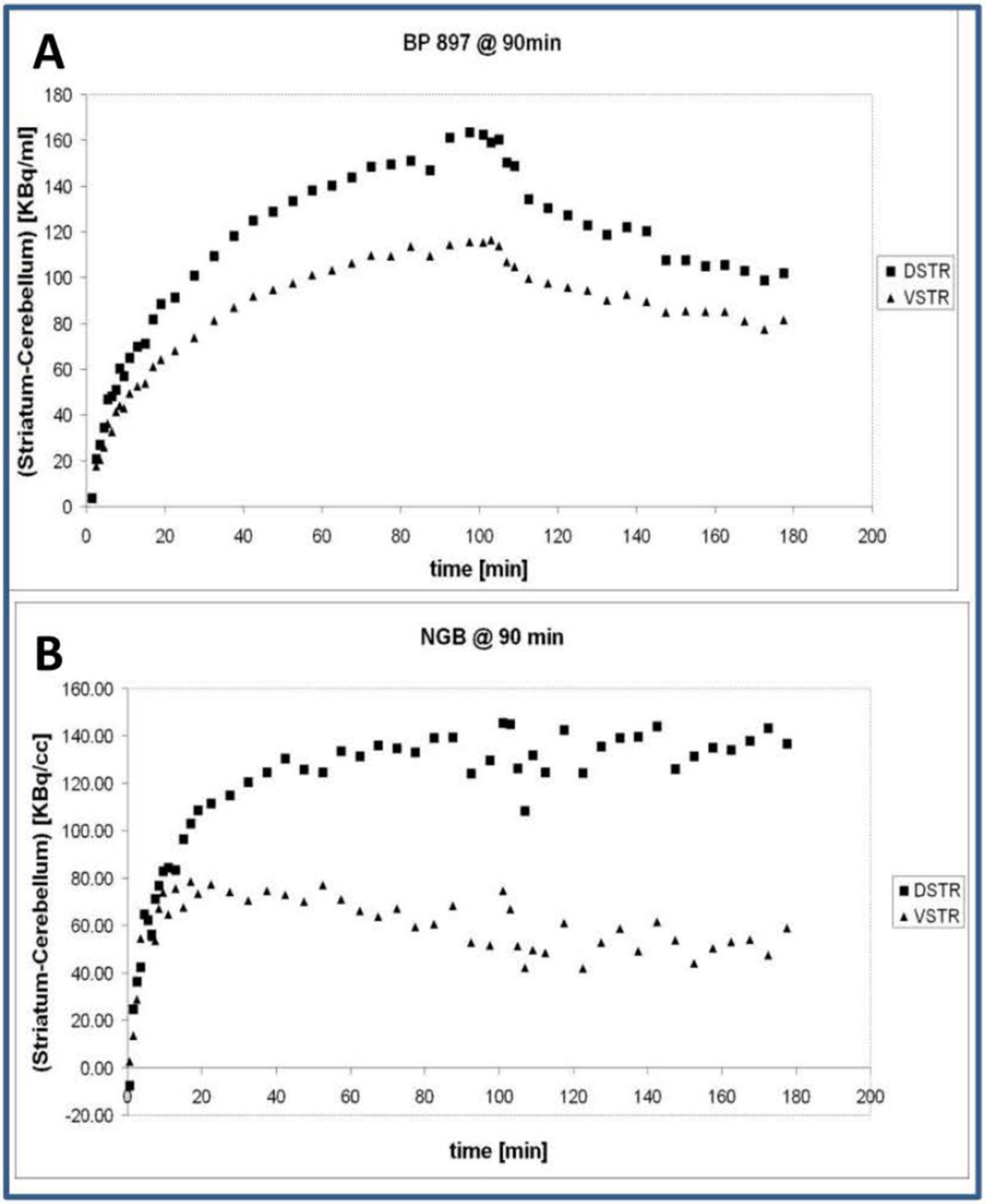

Figure 5.

(A) Effect of BP 897 on ^{18}F-fallypride binding in DSTR and VSTR, total 180 minutes of PET scanning shown, injection of BP 897 (3.2 mg/kg) occurred at 90 minutes. BP 897 causes a visible reduction in ^{18}F-fallypride binding. (B) Effect of NGB 2904 on ^{18}F-fallypride binding in dorsal striatum (DSTR) and ventral striatum (VSTR), total 180 minutes of PET scanning shown, injection of NGB 2904 (4 mg/kg) occurred at 90 minutes. NGB 2904 causes no measureable reduction in ^{18}F-fallypride binding.

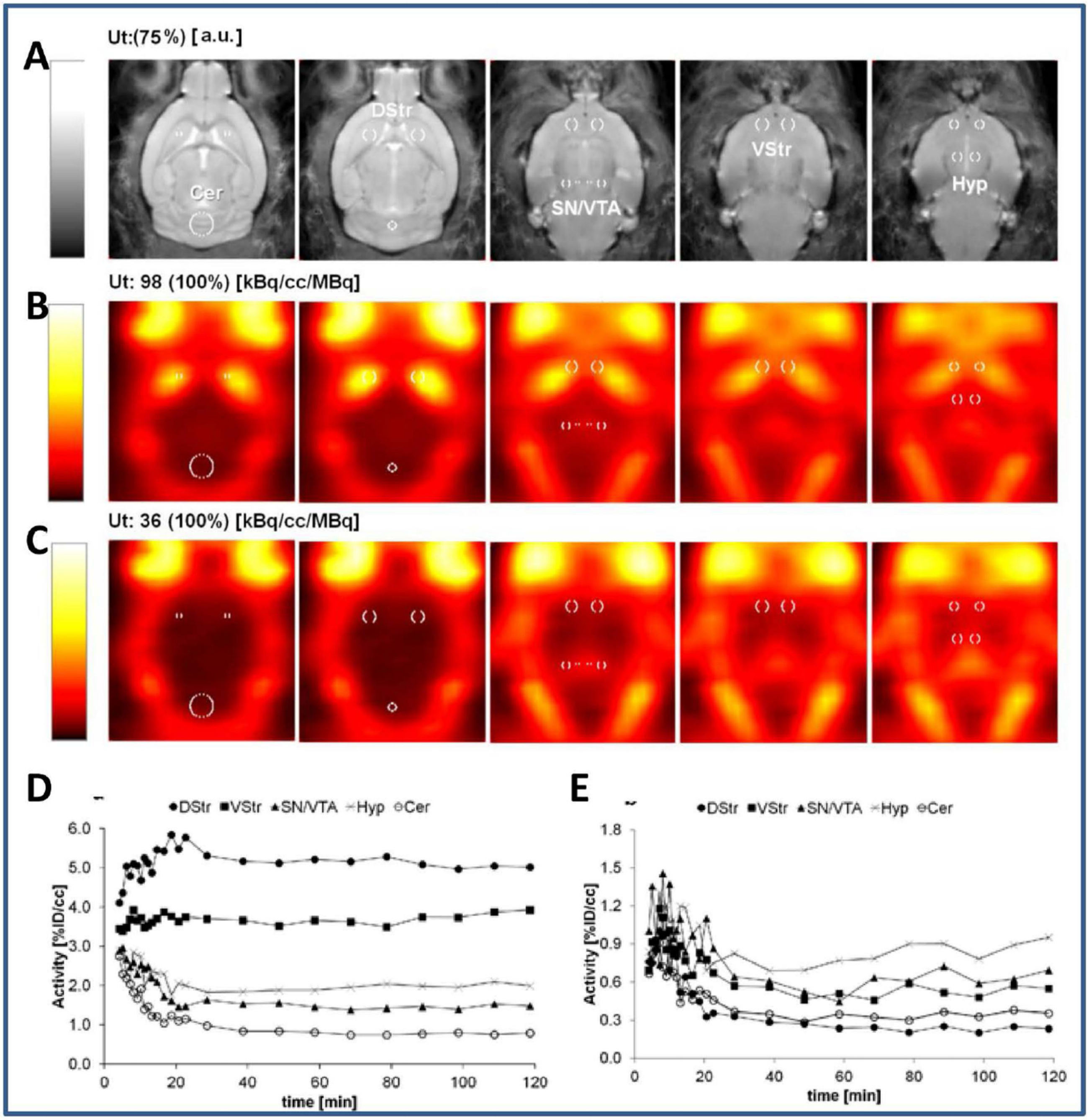

Figure 6.

In vivo PET images of ^{18}F-fallypride in wild-type (WT) and D2R knock-out (KO) mouse brain. Representative horizontal sections of (A) mouse brain MR template, ^{18}F-fallypride PET of the (B) WT, and (C) D2R KO. Dorsal-ventral coordinates with respect to the top of the image volume are −3.4 (left-most panel), −3.9, −5.5, −5.8 and −6.1 (right-most panel) mm. PET images were integrated over 20–120 min interval and divided by the total time and injected activity (in MBq). VOIs drawn on the MR template for cerebellum (Cer), dorsal striatum (DStr), substantia nigra\ventral tegmental area (SN\VTA), ventral striatum (VStr) and hypothalamus (Hyp) are shown in each panel, with labels on MR template. Legend: a.u. = arbitrary units, Ut = upper threshold. Representative time activity curves normalized to the injected dose of ^{18}F-fallypride from the WT (D) and D2 KO (E) mouse brain, respectively.

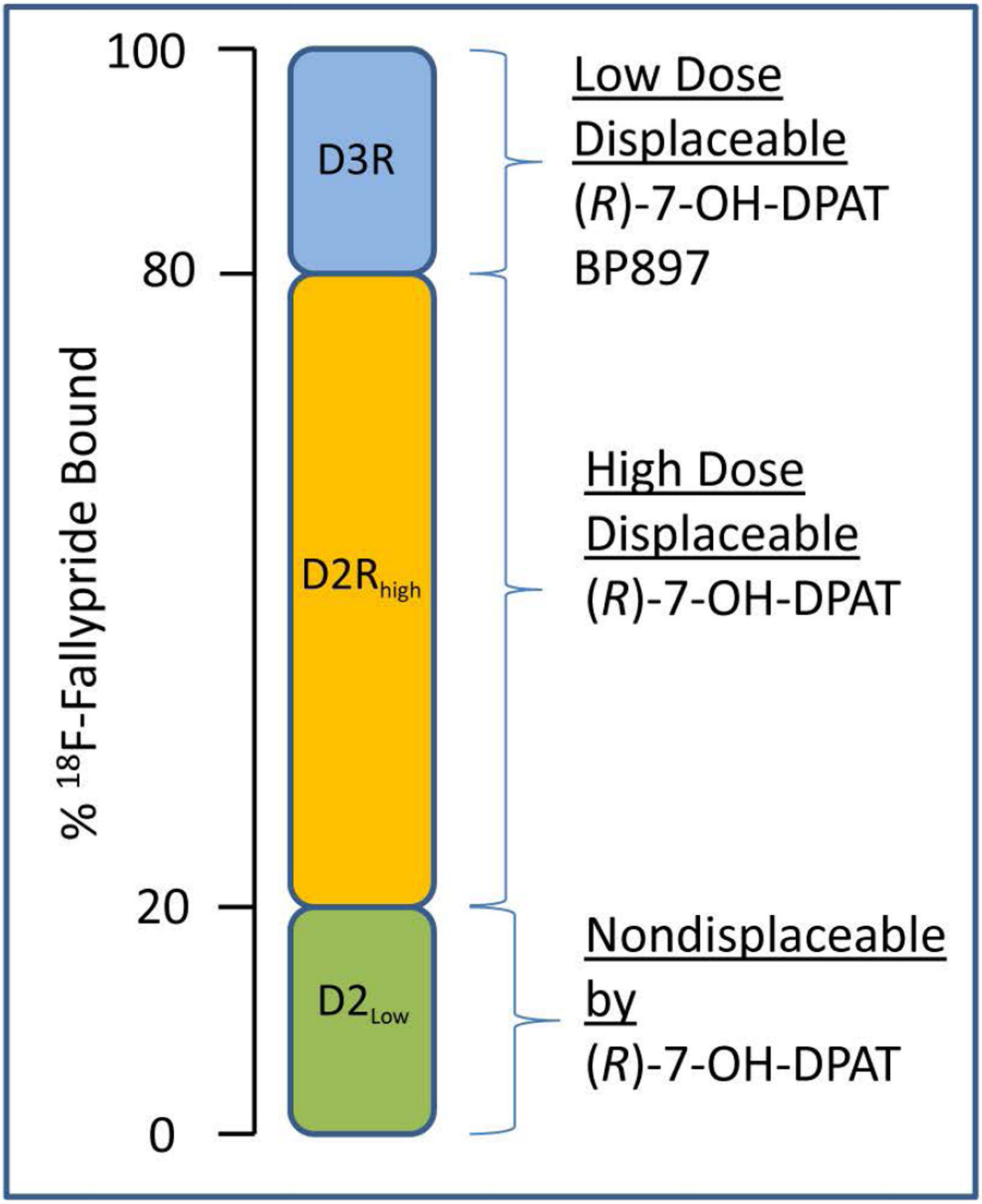

Figure 7.

Schematic showing approximate levels of ^{18}F-fallypride bound to dopamine D3R (20%), $D2R_{high}$ (60%) and $D2R_{low}$ (20%) receptors in the brain. The levels are approximately assessed primarily from the drug displacement studies reported here and emphasize the striatum.

Author Manuscript

Author Manuscript

Author Manuscript

Table 1

Binding Affinity (nM) of Drugs Used in the Study*

Drug	D2 Receptor	D3 Receptor	In Vitro D3 Selectivity	Comments
Fallypride[1]	0.05	0.30	0.17	Antagonist
Fallypride[2]	2.1	1.6	1.3	
(*S*)-7-OH-DPAT[3]	1780 (4777)[4]	55.6 (58)[4]	32	Agonist
(*R*)-7-OH-DPAT[3]	89 (56)[4]	2.4 (0.57)[4]	37 to 98	
(*RS*)-7-OH-DPAT[5]	61	0.78	78	
BP897[6]	61	0.9	68	Partial Agonist
NGB2094[6]	112	2.0	56	Antagonist
PHNO[7]	8.5 (0.24)	0.16 (0.6)	53	Agonist

*All affinities were measured in vitro.

[1]Mukherjee et al., 1999 (rat brain homogenates for D2R and cell lines for D3R using ^{3}H-spiperone;

[2]Stark et al., 2007;

[3]Lejeune et al., 1997;

[4]van Vliet et al., 1996;

[5]Gonzalez and Sibley, 1995;

[6]Heiderbreder et al., 2010;

[7]PHNO was not used in the study but is included to compare with the other drugs; Willeit et al., 2006.

Table 2

^{18}F-Fallypride Displacement *In Vivo* by Drugs Measured by PET*

Experimental Drug	Dose	Dorsal Striatum[3]	Ventral Striatum[3]	Nondisplaced ^{18}F-Fallypride	Anticipated Receptor Subtype Displaced
(*R*)-7-OH-DPAT[1]	0.015 mg/kg	−21.5%	−28.7%	71 to 78%	D3R
(*R*)-7-OH-DPAT[1]	0.06 mg/kg	−32.9%	−43.4%	57 to 67%	D3R+D2high
(*R*)-7-OH-DPAT[1]	0.38 mg/kg	−67.9%	−75%	25 to 32%	D3R+D2high
(*R*)-7-OH-DPAT[1]	1.88 mg/kg	−57.6%	−76.7%	23 to 42%	D3R+D2high
BP897[2]	3.2 mg/kg	−29.3%	−24.0%	70 to 76%	D3R
NGB2904[2]	4.0 mg/kg	Not significant	Not significant	100%	No displacement BBB impermeability?

[*] All drugs were injected intravenously 90 mins post-^{18}F-fallypride administration, while the rat was in the PET scanner.

[1] *R*)-7-OH-DPAT injected in sterile saline;

[2] BP897 and NGB2904 injected with 2-hydroxypropyl-β-cyclodextrin as described previously.

[3] Change measured from displacement curves shown in Figs 4 and 5.

Author Manuscript

Author Manuscript

Author Manuscript

Table 3

^{18}F-Fallypride Binding in D2R Knock-out mice*

	PET Measures		
	BP_{ND}		**fD3 %**
	WT	KO	
Dorsal Striatum	5.30	0	0
Ventral Striatum	3.51	0.55	15.6
Substantia nigra/ Ventral tegmental area	0.81	0.81	99.2
Hypothalmus	1.38	1.36	98.5

*Wild-type (WT) and D2R knock-out (KO) mice (BPND = binding potential nondispalcebale; fraction of total binding to D3 receptors, f_{D3}).

Table 4

In Vitro and *In Vivo* Imaging Evidence of D3R

Experiment	Radiotracer	Findings	Reference
D3R antibody immunostaining *In Vitro*	none	D3R mRNA and D3R antibody staining in islands of Calleja and low levels in nucleus accumbens and lateral septal nuclei.	Guo et al., 1998 Diaz et al., 2000
In Vitro	^{3}H-7-OH-DPAT	D3R binding at low concentrations and $D2R_{high}$ at higher concentrations	Gonzalez and Sibley, 1995
In Vitro	^{3}H-PD 128907	D3R binding; $D2R_{high}$ binding not known	Levant 1998
In Vitro and *In Vivo* PET	^{3}H/^{11}C-PHNO	D3R and $D2R_{high}$	Baba et al., 2015 Kiss et al 2011
In Vitro	^{125}I-7-OH-PIPAT	D3R binding; $D2R_{high}$ binding not known	Mugnani et al., 2013; Gurevich and Joyce, 1999
In Vitro and *In Vivo* PET	^{18}F-7-OH-FHXPAT	D3R binding; $D2R_{high}$ binding not known	Majji et al., 2012
In Vitro and *In Vivo* PET	^{11}C-5-OH-DPAT ^{18}F-5-OH-FPPAT	$D2R_{high}$ and some D3R (yet to be confirmed)	Mukherjee et al., 2000; Shi et al., 2004
In Vitro and *In Vivo*	^{3}H-LS-3–134	Ki D3R=0.17 nM (Partial agonist) B_{max} striatum=54 fmol/mg; nucleus accumbens =100 fmol/mg tissue.	Rangel-Barajas et al., 2014; Mach et al., 2011
In Vitro and *In Vivo* PET	^{18}F-Fallypride	~ 20% D3R ~ 60% $D2R_{high}$ ~ 20% $D2R_{low}$	In vivo levels in striatum (this paper)